

Impact of Metal, Oxide, and Hybrid Metal-Oxide Interlayers on Spin-Hall Effect in BiSb Topological Insulator and Magnetic Interfaces

Zhang Ruixian¹, Quang Le², XiaoYong Liu², Lei Xu², Brian R. York¹, Cherngye Hwang¹,
 Son Le², Maki Maeda³, Tuo Fan³, Yu Tao³, Hisashi Takano³,
 Min Liu¹, Shota Namba¹, Pham Nam Hai¹

¹Department of Electrical and Electronic Engineering, Institute of Science Tokyo, Tokyo 152-8552, Japan
²Western Digital Corp., Great Oaks site, San Jose, CA 95119, USA, quang.le@wdc.com
³Western Digital Corp., Fujisawa site, Kanagawa 252-0811, Japan
 Email: zhang.r.an@m.titech.ac.jp

The charge-to-spin conversion efficiency at the interface between a topological insulator (TI) and a ferromagnetic (FM) layer can be enhanced by inserting an interlayer (ITL). However, the mechanism of this enhancement is unclear. In this work, we systematically investigate the ITL effects by introducing various metals, oxides, and hybrid metal/oxide ITL between a BiSb topological insulator and a CoFe ferromagnetic layer. Our findings revealed that using a metallic NiFeGe or insulating MgO ITL resulted in similarly high efficiencies, with the highest efficiency achieved when employing hybrid NiFeGe/MgO ITL. However, efficiency decreased when NiFeGe was combined with MgTiO with increasing TiO composition. Such behaviors can be qualitatively understood by considering the ITL intrinsic effect of enhancing the intrinsic spin Hall angle of BiSb via preventing Sb diffusion from BiSb and migration of the FM, and the extrinsic effect where the ITL spin transparency is determined by the spin tunneling/diffusion across the ITL and the spin-flip/spin-transfer at the ITL/FM interface. This study provides valuable insights and a framework for understanding and optimizing interlayer materials for ultralow power spin-orbit torque applications.

Index Terms—Topological insulator, spin Hall effect, spin-orbit torque, SOT-MRAM, interfacial effect, spin tunneling, spin diffusion.

I. INTRODUCTION

Recently, several topological quantum materials with nontrivial band structures, such as Bi_2Se_3 ,¹ $(\text{Bi,Sb})_2\text{Te}_3$,² and BiSb^3 topological insulators (TIs) and YPtBi topological semimetals (TSM)⁴ have shown such a giant θ_{SH} . Among them, BiSb has attracted considerable attention as a promising SOT material candidate for future energy-efficient SOT device applications because it shows both giant room-temperature θ_{SH} and high electrical conductivity, and industrial tools can deposit it. However, the research on this BiSb material is still in its early stages, and the related physical, material, and device optimization remain to be addressed.

In this work, we aim to investigate and compare the effects of inserting metal, oxide, and hybrid metal-oxide interlayers between the BiSb and FM layer. We not only observe how effectively they can enhance the charge-to-spin conversion efficiency but also study the mechanism behind their effects. To determine the interlayers' relative efficiency, we evaluate their dampinglike SOT efficiency per unit current density, ξ_{DL}^j , or effective spin Hall angle $\theta_{\text{SH}}^{\text{eff}}$, which is a function of the product of T_{IST} , the interfacial spin transparency, and θ_{SH} , the intrinsic spin Hall angle, as given by Eq. 1,⁵

$$\xi_{\text{DL}}^j \equiv \theta_{\text{SH}}^{\text{eff}} = T_{\text{IST}} \theta_{\text{SH}} \quad (1)$$

Then, we explain the impact of each type of interlayer on ξ_{DL}^j . Our study can provide a useful framework for understanding ultrahigh ξ_{DL}^j and guidance on increasing it by optimizing the TI's interlayer material for ultralow power SOT applications.

II. EXPERIMENT PROCEDURE

The whole BiSb stack consists of a buffer, a 10 nm BiSb layer, a matrix of interlayers by wafer, a ferromagnetic (FM) 0.7 nm $\text{Co}_{40}\text{Fe}_{60}$ layer, and a capping layer that was deposited at room temperature on a silicon oxide substrate after a conventional cleaning process, followed by a light sputter etch inside a physical vapor deposition tool. The buffer and matrix of the interlayers are designed to promote BiSb (012) orientation, prevent migration and Sb diffusion, and offer greater resistivity than BiSb to minimize shunting. A series of interlayer materials, including metals, oxides, and hybrid metal/oxides such as NiFeGe, MgO, NiFeGe/MgO, and NiFeGe/MgTiO were incorporated into the BiSb stacks for a comparative analysis of their effectiveness on ξ_{DL}^j and impact on θ_{SH} and T_{IST} . Structural, thickness, composition, and orientation characterization of the BiSb stacks with a matrix of interlayers were confirmed by using XRR, XRF, and XRD data, and TEM image. Figure 1

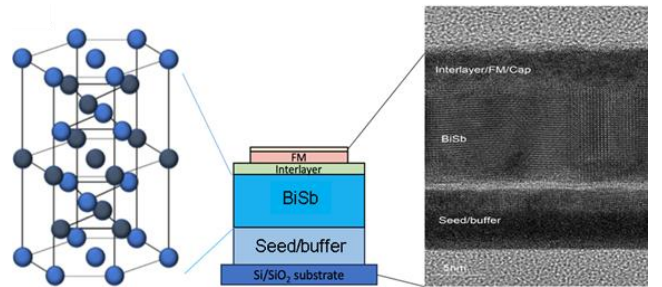


Figure 1. The representative BiSb stack consists of seed/buffer layers, a 10 nm BiSb layer, a matrix of interlayers by wafer, an FM layer, and a capping layer deposited at room temperature.

shows a typical stack structure and cross-section TEM.

In this work, ξ_{DL}^j is obtained by exploiting the second harmonics Hall technique. An AC is applied in-plane to the BiSb/FM Hall bar, generating an alternating pure spin current due to the spin Hall effect. This spin current diffuses to the adjacent FM layer across the interface, subsequently exerting an SOT on the FM layer. Consequently, the FM's oscillation as the result of the SOT gives rise to the second harmonic Hall voltage response, which is characterized by Eq. 2 for the case of in-plane magnetization,

$$R_H^{2\omega} = \frac{R_{AHE}}{2} \left(\frac{H_{AD}}{H_k + H_x} \right) + \alpha_{ONE} H_x + R_{ANE+SSE}, \quad (2)$$

where $R_H^{2\omega}$ is the second harmonic Hall resistance, R_{AHE} is the anomalous Hall resistance, H_{AD} is the anti-damping like field, H_k is the effective magnetic anisotropy field, H_x is the in-plane applied magnetic field, α_{ONE} is the ordinary Nernst effect coefficient, and $R_{ANE+SSE}$ is a constant representing contribution of the anomalous Nernst effect and spin Seebeck effect.

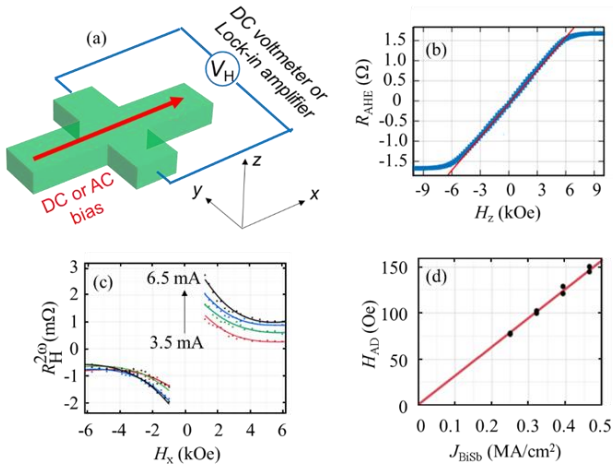


Figure 2. Representative measurement of a sample with a 10 nm-thick BiSb layer, a 1.2 nm MgO interlayer, a 0.7 nm-thick CoFe FM layer. (a) Illustration of the measurement circuit. (b) Anomalous Hall resistance measured with a perpendicular magnetic field. (c) Second harmonic Hall resistance (points) and the corresponding fitting (solid lines). (d) Damping-like field H_{AD} as a function of the current density J_{BiSb} in BiSb.

Figure 2(a) illustrates the measurement circuit using Hall bar devices. The fabricated Hall bar devices have four terminals and measures $10 \times 25 \mu\text{m}^2$. We first measured R_{AHE} and H_k with a DC bias and a perpendicular magnetic field. Then, we measure $R_H^{2\omega}$ while sweeping an in-plane magnetic field along the x direction. We then fit the $R_H^{2\omega} - H_x$ data into Eq. 2 to estimate H_{AD} and plot H_{AD} as a function of the current density inside BiSb, J_{BiSb} . Finally, we estimate ξ_{DL}^j from the slope of $\frac{H_{AD}}{J_{BiSb}}$ as shown in the following Eq. 3:

$$\xi_{DL}^j = (2e/\hbar) M_S t_{FM} \frac{H_{AD}}{J_{BiSb}}, \quad (3)$$

where M_S is the measured saturation magnetization of the FM layer, and $t_{FM} = 0.7 \text{ nm}$ is its thickness.

III. ξ_{DL}^j OF METALS, OXIDES, AND HYBRID METAL-OXIDES INTERLAYERS

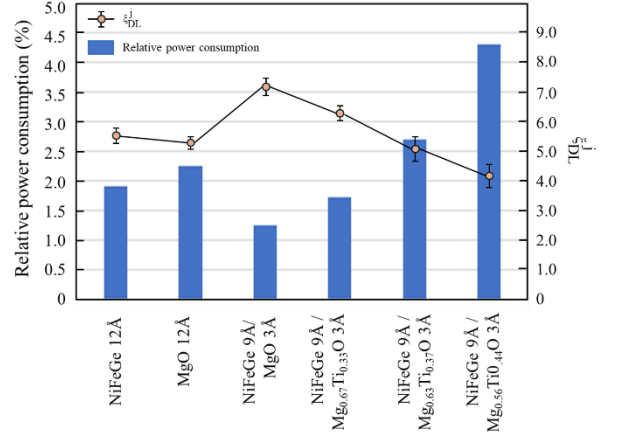


Figure 3. ξ_{DL}^j as the function of metal, oxide, and hybrid metal/oxide interlayers and power consumption as the function of interlayers, relative to that of Ta.

Figure 3 shows ξ_{DL}^j and relative power consumption of sample A₁ with a NiFeGe (12 Å) ITL, sample A₂ with an MgO (12 Å) ITL, sample B with a hybrid NiFeGe (9 Å) /MgO (3 Å) ITL, and samples C₁-C₃ with a NiFeGe (9 Å) /Mg_{1-x}Ti_xO (3 Å) ITL whose x was 0.33, 0.37, and 0.44, respectively. We normalized the power consumption by that of a reference sample with a 10 nm-thick Ta layer, which shows $\xi_{DL}^j = 0.18$. A closer examination of Fig. 3 reveals a large ξ_{DL}^j , small relative power consumption in the samples A₁ and A₂ with NiFeGe and MgO ITL, while the maximum ξ_{DL}^j and minimum relative power consumption is achieved in the sample B with the hybrid NiFeGe/MgO ITL, and it decreases in samples C₁-C₃ with the NiFeGe/MgTiO ITL whose TiO concentration gradually increases. In comparison, we only observed ξ_{DL}^j of 0.2 for the sample N without an ILT. This result clearly shows that selecting an optimal interlayer can effectively tune θ_{SH} and the spin transmission into the FM layer and hence ξ_{DL}^j .

We thoroughly studied the impact of different metal, oxide, and hybrid metal/oxide interlayers on the charge-to-spin conversion efficiency of BiSb thin films. Our findings revealed that utilizing a NiFeGe or MgO interlayer resulted in nearly the same high efficiency, with the highest efficiency achieved when using hybrid NiFeGe/MgO interlayers. However, efficiency decreased when NiFeGe was combined with MgTiO with increasing TiO composition. Such behaviors can be qualitatively understood by considering the ITL intrinsic effect of enhancing the intrinsic θ_{SH} via preventing Sb diffusion from BiSb and migration of the FM.

REFERENCES

- [1] A. R. Melnik, et al. Nature 511, 449 (2014).
- [2] H. Wu, P. Zhang, P. Deng, Q. Lan, Q. Pan, S. A. Razavi, X. Che, L. Huang, B. Dai, K. Wong, X. Han, K. L. Wang, Phys. Rev. Lett. 123, 207205 (2019)
- [3] N. H. D. Khang, Y. Ueda, P. N. Hai, Nat. Mater. 17, 808 (2018).
- [4] T. Shirokura, T. Fan, N.H.D. Khang, T. Kondo, P. N. Hai, Sci. Rep., 12, 2426 (2022).
- [5] L. Zhu, D. C. Ralph, R. A. Buhrman, Phys. Rev. B 99, 180404(R) (2019)